Received: 3 June 2017 | Revised: 27 July 2017 | Accepted: 28 July 2017

DOI: 10.1002/aoc.4056

FULL PAPER

WILEY Applied Organometallic Chemistry

Catalytic reactivity of new Ni(II), cu(II) and Sn(II) complexes for decolorization of indigo carmine in aqueous solution, high efficiency of copper complex

Amr Mohammad Nassar[1,2]

[1] Chemistry Department, College of Science, Aljouf University, PO Box 2014 Sakaka, Aljouf, Saudi Arabia

[2] Chemistry Department, Faculty of Science, Al-Azhar University, Nasr city, 118804, Cairo, Egypt

Correspondence
Amr Mohamed Nassar, Chemistry Department, College of Science, Aljouf University, Sakaka, Aljouf, Saudi Arabia.
Email: nassar_tanta@yahoo.com

A new Ni(II), Cu(II) and Sn(II) Schiff base complexes were synthesized in this work. The characterization of the new complexes is carried out by elemental analysis, FT-IR, UV–Visible, ^{1}H NMR and ^{13}C NMR spectroscopy, conductance analysis, magnetic measurements and thermal gravimetric analysis. It was found that the ligand behaves as a dibasic bidentate which coordinated to the metal center through two deprotonated hydroxyl groups to form tetrahedral complex with Ni(II) and octahedral complex with Cu(II). The ligand acts as neutral bidentate through azomethine nitrogen and thiazol sulfur to form octahedral complex with Sn(II). The synthesized complexes are evaluated as catalysts for oxidative degradation of indigo carmine dye using H_2O_2 as oxidant and the efficiency of the catalysts is determined. The copper complex shows the best catalytic action with efficiency 92.17% after 25 min.

KEYWORDS
catalysts, complexes, degradation, indigo carmine, oxidation

1 | INTRODUCTION

Schiff bases have excellent coordinative capability to form stable complexes with most of metal ions.[1] The wide range of applications of these complexes were studied by several works.[2–7] From these applications, A large number of Schiff base complexes exhibit remarkable catalytic activity for enhancing yield and product selectivity. Schiff base complexes show excellent homogeneous and heterogeneous catalytic properties in various reactions such as oxidation of organic compounds,[8] reduction of alkyl and aryl halides,[9] DNA bending,[10] H_2O_2 decomposition,[11] ester hydrolysis[12] and dyes decolonization from aqueous solutions.[13,14] Indigo Carmine is one of the mainly dyes used in the textile dyeing. It is also used in food, cosmetics, paper, and plastics as coloring dye, redox indicator in analytical chemistry, and in biology microscopic stain.[15] It is found that, the effluent from textile dying industry contain about 30% of the applied dyes remain unfixed and are discharged in the wastewater.[16] Indigo Carmine is highly toxic, cause eye and beings irritations to human and leads to tumors at the site of application.[17] It makes the removal of indigo carmine from industrial wastewater be a major concern for the human health and environmental standpoint. Hydrogen peroxide is environmental friendly oxidizer because it produces H_2O and O_2 as a final reduction products. Also, it is available and cheap reagent.[18] H_2O_2 without catalyst is moderate oxidizing agent of organic compounds while in the presence of catalyst, photo, ultrasound or heat, lead to powerful oxidation and degrade many organic substrates.[19] The using of H_2O_2 in the degradation of different organic dyes and their color removal from industrial wastewater effluents have been studied.[20–22] Moreover, the using of transition metal complexes as heterogeneous catalysts in decomposition of indigo carmine with H_2O_2 has been investigated.[23–25] In this work, the catalytic activity of newly synthesized Schiff base

complexes in degradation of Indigo Carmine was investigated. To the best of the author knowledge, this is the first report for the using of Schiff base complexes in catalytic removal of indigo carmine from aqueous solutions. This system may be apply to color removal in wastewater effluent stream.

2 | EXPERIMENTAL

2.1 | Materials and methods

Indigo Carmine dye was obtained from Sigma-Aldrich and used as received. Hydrogen peroxide (30%, *w*/*v*) was used as an oxidizer. All the chemical reagents were analytical grade and were used as received. All the experiments were done using MQ water. The solvents used in this work were extra-pure grades and were used as received.

2.2 | Instrumentation

Elemental analysis was detected using a CHNS-932 (LECO) Vario elemental analyzer. Room temperature magnetic susceptibility measurements were conducted with a Sherwood Scientific magnetic balance. UV–visible spectra in the range (195–1100 nm) were recorded using labomed Spectro UV–VIS Double PC 8 Auto cell scanning spectrophotometer.IR spectra were carried out using KBr pellets with a PerkinElmer 1430 spectrometer in the region 4000–200 cm^{-1}. The instrument used for performing the thermal gravimetric analysis (TGA) was TGA-50 Shimadzu thermogravimetric analyzer. ^{1}H NMR and ^{13}C NMR spectra were recorded with a GEMINI-300BB NMR 500 MHz spectrometer.

2.3 | Synthesis of metal complexes

Complexes 1, 2 and 3 were synthesized by dropwise addition of 50 ml of a methanolic solution of 0.0020 mol of each $NiNO_3.6H_2O$, $Cu(OAC)_2.H_2O$ and $SnCl_2.2H_2O$ respectively to hot stirred methanolic solution of H_2L (0.3 g, 0.0010 mol) (50 ml) in metal: ligand molar ratio of 2:1. Complexes 2 and 3 are precipitated immediately while complex 1 is precipitated after reflux 2 h then addition of 1.2 ml of deionized water. The metal complexes were filtered, washed several times with hot water and acetone then finally dried in oven at 110 °C. Below are mentioned the most important characteristics of the obtained complexes.

2.3.1 | Complex 1:

Deep green solid; m.p. > 300 °C; molecular weight 392.06 $g.mol^{-1}$. Anal. Calcd for $C_{15}H_{15}N_3NiO_4S$ (%): C, 45.95; H, 3.86; N, 10.72; Ni, 14.97. Found (%): C, 46.0; H, 4.0; N, 3.9; Ni, 15.0. Main IR peaks (KBr, cm^{-1}): 1601 (C=N), 745 ν C-S-C, 1162 (C—O), 3421 ($\nu_{as}H_2O$), 448 (Ni—O). $\Lambda m(\Omega^{-1}\ mol^{-1}\ cm^2)$: 4.55. UV–visible (DMF, nm): 671 nm (d–d transition). μ_{eff} (BM): 3.49 B.M.

2.3.2 | Complex. 2

Deep brown solid; m.p. > 300 °C; molecular weight 396.01 $g.mol^{-1}$. Anal. Calcd for $C_{15}H_{15}N_3CuO_4S$ (%):C, 45.39; H, 3.81; N, 10.95; Cu, 16.01. Found(%): C, 45.40; H, 3.75; N, 10.66; Cu, 16.02. Main IR peaks (KBr, cm^{-1}): 1601 (C=N), 746 ν C-S-C, 1177 (C—O), 3423 ($\nu_{as}H_2O$), 452 (Cu—O). $\Lambda m(\Omega^{-1}\ mol^{-1}\ cm^2)$: 5.02. UV–visible (DMF, nm): 433, 471, 580 and 822 nm (d–d transition). μ_{eff} (BM): 2.15 B.M.

2.3.3 | Complex. 3

Greenish yellow solid; m.p. > 300 °C; molecular weight 788 $g.mol^{-1}$. Anal. Calcd for $C_{30}H_{26}Cl_2N_6O_4S_2Sn$ (%): C, 45.68; H, 3.30; N, 10.65; Sn, 15.06. Found (%): C, 45.55; H, 3.35; N, 10.77; Sn, 15.10. Main IR peaks (KBr, cm^{-1}): 1588 (C=N), 700 ν C-S-C, 1183 (C—O), 3469 (ν OH), 452 (Cu—O). $\Lambda m(\Omega^{-1}\ mol^{-1}\ cm^2)$: 4.75. UV–visible (DMF, nm): 490 (charge transfer). μ_{eff} (BM): Diamagnetic. Main $^{1}HNMR$ signals, δ = 8.2 ppm (HC = N), 9–10.5 PPM (OH). Main $^{13}CNMR$ signals δ = 146,148 (C-OH), 158(Ph-C = N).

2.4 | Catalytic tests

The methods of Indigo Carmine degradation was carried out in a conical flasks (250 cm^3) containing a mixture of IC 1×10^{-4} M, $1cm^3H_2O_2$ solution and 0.02 gm catalyst equipped with a magnetic stirrer. The kinetic run was started from the addition of the catalyst. The mixture was continuously stirred at room temperature. At the suitable time intervals, the descending IC concentration is followed up by withdrawing a 5 cm^3 sample and filtration from the catalyst to stop the reaction. The absorbance of IC is recorded at λ_{max} using UV–VIS spectrophotometer between 190–1100 nm with a maximum absorbance at λ = 610 nm.[23] The efficiency of IC decolorization was determined by Equation 1.

$$\text{IC decolorization } (\%) = \frac{Ao - At}{Ao} \times 100 \qquad (1)$$

Where Ao is the value of absorbance at time 0 and At is the value of absorbance at any time t in min.

3 | RESULTS AND DISCUSSION

The Schiff base ligand, H_2L represents in Figure 1 was prepared and characterized according to literature.[26] The reaction of nickel (II), copper (II) and tin (II) salts with H_2L in molar ratios and 2: 1 (M: L) in methanol under refluxing conditions resulted in the formation of complexes 1 and 2 with stoichiometries 1: 1 and complex 3 in 1: 2 (M: L), respectively. As listed in experimental section, the complexes melt above 350 °C. The complexes are air stable, freely soluble in DMF and DMSO and only complex 1 is partially soluble in MeOH, EtOH. The molar conductance of 10^{-3} M solutions of the complexes in DMF clear that the complexes are non-electrolytes.[27]

3.1 | Characterization of the complexes

3.1.1 | IR spectra

The important infrared bands of the Schiff base and its transition metal chelates are collected in Table 1.

The IR spectrum of the ligand shows a characteristic band at 1601 cm^{-1} assignable to ν C = N, indicating the formation of Schiff base molecule. The weak bands observe at 3075 and 2924 cm^{-1} is attributed to stretching vibration of aromatic and aliphatic C-H, respectively. A sharp band observes at 3469 cm^{-1} is assignable to ν_{OH} groups. A medium intensity band observes at 744 cm^{-1} is due to ν C-S-C.[28] Also, stretching vibration of C-O represents a sharp band at 1183 cm^{-1}.

The IR spectra of complexe 1 and 2 do not exhibits appreciable change in position of the (C = N) band indicates the not participation of azomethine nitrogen in the chelation with metal ions. Also, the spectra of the complexes show a medium intensity band at 744 and 746 cm $^{-1}$ which is attributed to ν C-S-C. No change in the position of this band in the spectra of the ligand and the complexes which supports the S atom is not included in coordination with metal ions. Moreover, A sharp band observed in the range 1162 and1177 cm^{-1} which is due to a phenolic ν C-O stretching vibration. The shift of this band toward lower frequency in comparing with H_2L is assignable to the weakness of this bond after chelation of phenolic oxygen with metal ions.[29]

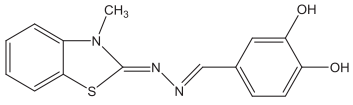

FIGURE 1 Structure of Schiff base ligand H_2L

The spectra of complexes 1 and 2 show a strong broadness band at 3421 and 3423 cm^{-1}, respectively which assignable to ν_{as} of coordinated H_2O molecules.[30] The far infrared region of the complexes display new shoulder at 448 and 452 cm^{-1} which is not found in the spectrum of the free ligand. This band is due to $\nu_{M\text{-}O}$.

Complex 3 shows a band at 1588 cm^{-1} assignable to azomethine stretching vibration. The shift of this band to lower frequency indicating the weakness of this group due to participation of azomethine nitrogen with Sn^{2+}.[31] Also the lower shift of ν C-S-C band to 700 cm^{-1} assignable to coordination of S atom with stannous ion. Confirming this, the appearance of new medium intensity bands at 507 and 369 cm^{-1} which are due to $\nu_{Sn\text{-}N}$ and $\nu_{Sn\text{-}S}$, respectively. The broad band at 3423 cm^{-1} is attributed to stretching vibration of phenolic OH. The band observes at 308 cm^{-1} in the spectrum of complex 3 is assignable to $\nu_{Sn\text{-}Cl}$.

Accordingly, the ligand H_2L acts as a dibasic bidentate ligand coordinated to the Ni(II) and Cu(II) ions as $-O^-$ in these complexes and a neutral bidentate ligand coordinated to Sn(II) ion through N and S.

3.1.2 | UV–vis spectra and magnetic susceptibility measurements

The electronic spectra of the Schiff base ligand H_2L and its metal complexes were recorded in DMF solution, Table 2. The ligand shows bands at 324 and 390 nm due to π-π^* transitions. In the spectra of the complexes, these bands slightly bathchromic shift that could be attributed to the complexation. The ligand chromophore C = N, which absorbs at 430 nm assignable to n-π^*transition is not shifted in the spectra of the complexes 1 and 2 but shifts to higher wavelength at 490 nm in the spectrum of complex 3 possibly due to polarization of the C = N bond produced from the metal–ligand interaction.[32] In addition the spectra displays new bands above 500 nm due to d-d transition.

TABLE 1 Infrared spectral analysis of ligand(H_2L)and its complexes

Compound	$\nu_{C=N}$	$\nu_{C\text{-}S}$	$\nu_{C\text{-}O}$	ν_{OH}	$\nu_{M\text{-}O}$	$\nu_{M\text{-}N}$	$\nu_{M\text{-}S}$	$\nu_{M\text{-}Cl}$
Ligand H_2L	1601	744	1183	3469	-	-	-	-
Complex 1 $[Ni(L)(H_2O)_2]$	1601	745	1162	3421 (H_2O)	448	-	-	-
Complex 2 $[Cu(L)(H_2O)_4]$	1601	746	1177	3423 (H_2O)	452	-	-	-
Complex 3 $[Sn(H_2L)_2Cl_2]$	1588	700	1183	3469 (Phenolic)	-	507		

TABLE 2 Electronic spectral analysis and magnetic measurements of complexes

Compound	Bands (nm)	Interpretation	Magnetic susceptibility (B.M)	Geometrical structure
Ligand H_2L	324,390	π-π^*	-	-
	430	n- π^*		
Complex 1 $[Ni(L)(H_2O)_2]$	430	n- π^*	3.49	Tetrahedral
	671	$^3T_1(F) \rightarrow {}^3T_1(P)$		
Complex 2 $[Cu(L)(H_2O)_4]$	433	n- π^*	2.15	Octahedral
	822	$^2B_{1g} \rightarrow {}^2A_{1g}$		
	580	$^2B_{1g} \rightarrow {}^2B_{2g}$		
	471	$^2B_{1g} \rightarrow {}^2E_g$		
Complex 3 $[Sn(H_2L)_2Cl_2]$	490	C.T*	D**	Octahedral

*Charge transfer

**Diamagnetic

The UV–Vis spectrum of complex 1 exhibits a broad band at 671 nm corresponding to $^3T_1(F) \rightarrow {}^3T_1(P)$ indicates the tetrahedral arrangement of the ligand surrounding Ni(II) in this complex. The magnetic moment value of 3.49 BM is in the range of 3.2–4.0 BM expected for the tetrahedral Ni(II) complexes.[33]

The μ_{eff} of complex 2 is 2.15 B.M., which confirms the octahedral structure of this complex. The electronic spectrum of the complex, Figure 2 shows a bands at 822, 580 and 471 nm, which are attributed to $^2B_{1g} \rightarrow {}^2A_{1g}$, $^2B_{1g} \rightarrow {}^2B_{2g}$ and $^2B_{1g} \rightarrow {}^2E_g$ transitions, respectively. The band observed at 433 nm indicating the existence of a transition from dxy,dxz, dyz and $dz^2 \rightarrow$ antibonding dx^2-y^2 which is half-filled level, this is consistent with an six coordinated configuration.[34]

The complex 3 is diamagnetic and its electronic spectrum shows one broad bands in the region 490 nm which may be assigned as charge transfer. It was reported that the metal is capable of forming dπ–pπ* bonds with ligands containing nitrogen as the donor atom. The d orbital of Sn atom has 5d completely vacant, so the nitrogen-metal coordination bond can formed by the acceptance of the nitrogen lone pair of electrons.[35]

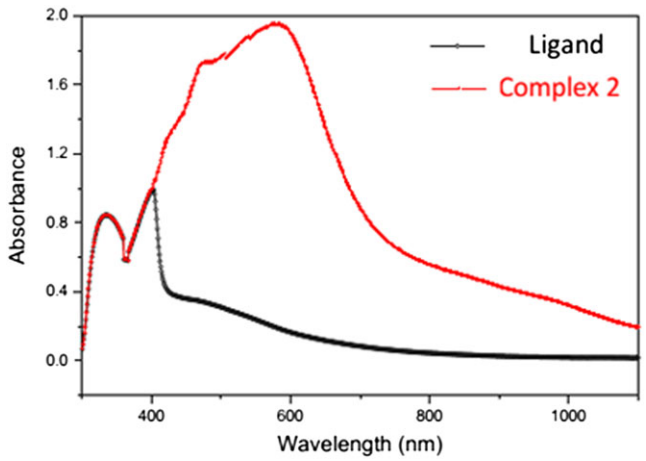

FIGURE 2 Electronic spectra of ligand and complex 2

3.1.3 | Thermal gravimetric analysis

The thermograms of Schiff base ligand shows the first step of decomposition within the temperature range (25-275 °C) attributed to liberation of $C_7H_6O_2$ as gases with mass loss of 40.88% (calc: 40.80%). The remaining steps show the complete degradation of the organic part $C_8H_7N_3S$ within the temperature range (275–700 °C) with estimated mass loss 59.12% (calc: 59.20%).

The TGA figure of complex 1 displays four steps of decomposition. The first and second steps within the temperature range 25–180^0 C correspond to elimination of three NH_3 molecules with founded mass loss 12.95% (calc: 13.01%). The third step of thermal decomposition 180–250 °C is corresponds to the loss of two coordinated water molecules with a mass loss 9.10% (calc: 9.18%). The fourth step is matching with the loss of the organic part of Schiff base ligand $C_{15}H_2O_2$ with mass loss 54.70% (calc: 54.59%) leaving NiS as residue 23.34% (calc: 23.19%).

Complex 2 decomposed in four decomposition steps. The first and second decomposition steps occurred in the range 25–225 °C assigned to loss of N_2 molecule with estimated mass loss 6.59% (calc: 6.47%). The third decomposition stage revealed in the range 225-315 °C which can be attributed to loss of NH_3,$4H_2O$ and O_2 and organic part C_8H_{11} with estimated mass loss 52.89% (calc: 52.65%). The last weight loss stage appeared in the range 315–675 °C produced CuS as residue 22.31% (calc: 22.05%).

Complex 3 is thermally decomposed in two steps. One molecule of Cl_2 gas is loosed in the first step in the temperature range 25–300 °C with estimated mass loss 8.46% (calc: 8.84%). The second step shows the loss of the organic moiety within the temperature range 300–570 °C corresponds to mass loss 72.30% (calc: 72.47%).

The residual part of TGA of this complex is found to be SnS, 18.46% (calc: 18.68%).

3.1.4 | ^{1}HNMR and ^{13}CNMR spectra

The ^{1}HNMR and ^{13}CNMR spectra of complex 3 are recorded in DMSO-*d6* and compared with that of the free Schiff base ligand reported in previous work.[26]

In the ^{1}H NMR spectrum of Sn(II) complex, Figure 3, the azomethine proton signal is slightly shifted to downfield and appeared at 8.2 ppm. This shift in azomethine proton position could assignable to the coordination of azomethine nitrogen atom with metal ion.[36] The aromatic signals appeared slightly deshielding due to increased conjugation upon coordination.[37] The broad and weak signals appeared in the range 9–10.5 ppm are attributed to hydroxyl protons which indicates that the hydroxyl groups are not participate in the coordination with stannous ion. These signals are disappeared when D_2O is added to the solution due to proton exchangeable, Figure 4.

The ^{13}CNMR spectrum of tin complex, Figure 5, shows two signals at 146.0 and 148.3 ppm which are due to C-OH. No remarkable shift in this signals when

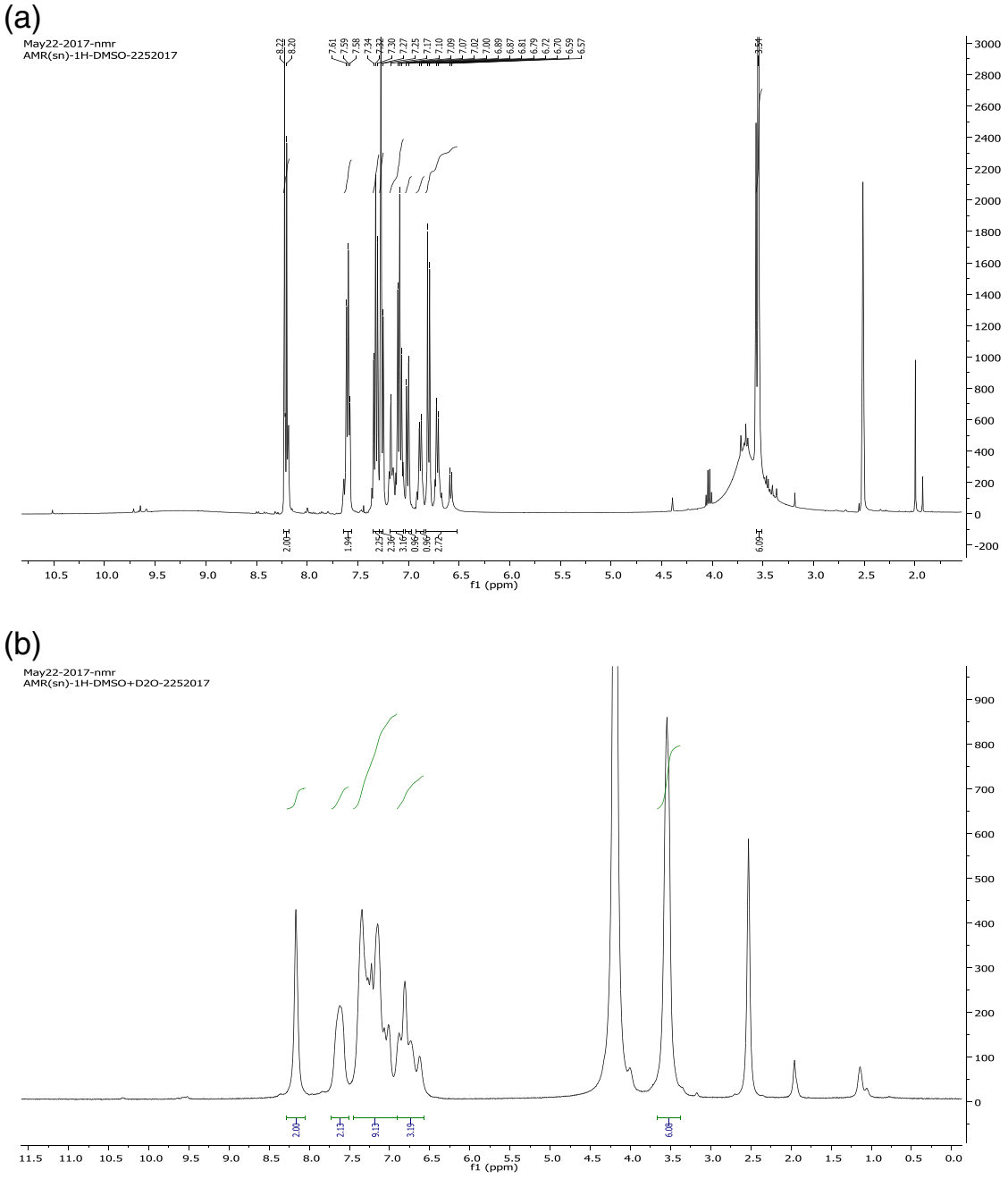

FIGURE 3 ^{1}HNMR spectrum of complex 3 in DMSO. ^{1}HNMR spectrum of complex 3 in DMSO + D_2O

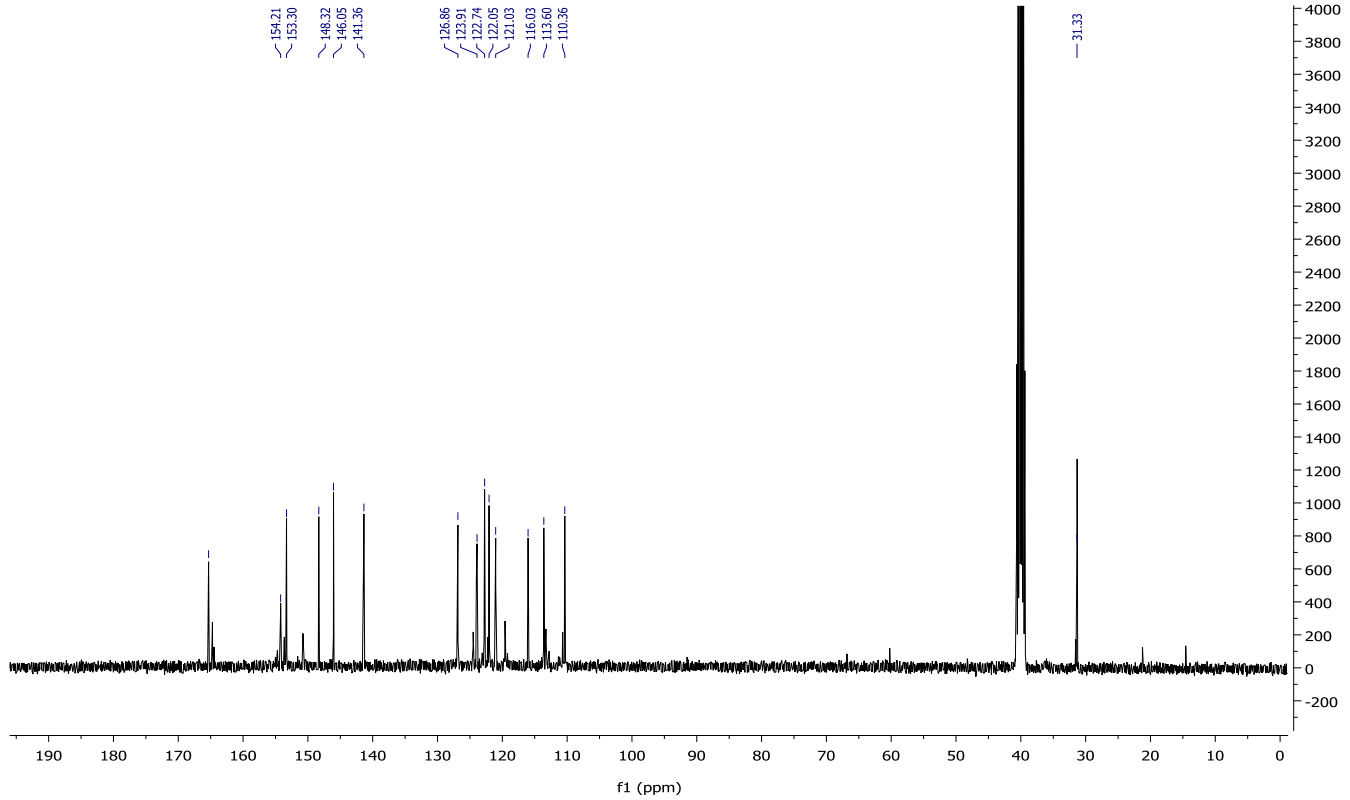

FIGURE 4 ^{13}CNMR spectrum of complex 3 in DMSO

compared with the spectrum of the ligand. This result confirms that the hydroxyl groups are not included in complexation with tin. On the other hand the signal due to Ph-C = N- is appeared at 158 ppm. This signal are slightly shifted to down field region when compared with that of free ligand indicating the involvement of azomethine nitrogen in coordination with Sn^{2+}.

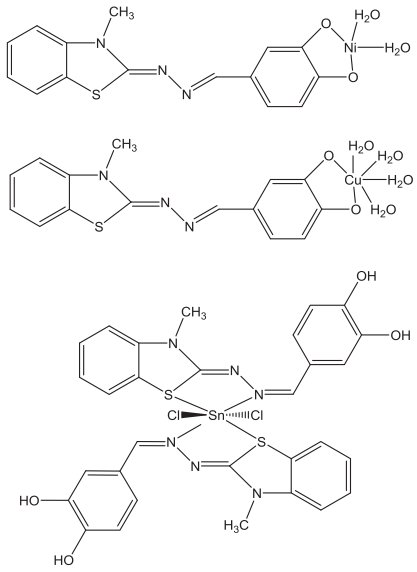

FIGURE 5 Proposed structure of the metal complexes

Consequently, the proposed structure of the synthesized metal complexes are shown in Figure 6.

3.2 | Catalytic activity of the complexes

In this part of study indigo carmine dye (IC) was chosen as a model to investigate its oxidative degradation by H_2O_2 as an oxidant using the synthesized metal complexes as catalysts.

Figure 7 shows the behavior of 1×10^{-4} M solution of indigo carmine, after 10 min from addition of H_2O_2 only without catalyst and H_2O_2 + 0.02 gm of different catalysts and the degradation is followed using UV–Vis spectrophotometer. When H_2O_2 solution was added to the dye

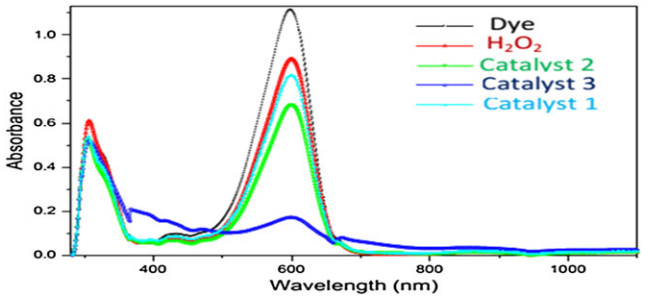

FIGURE 6 Degradation of indigo carmine without and with catalysts after 10 min

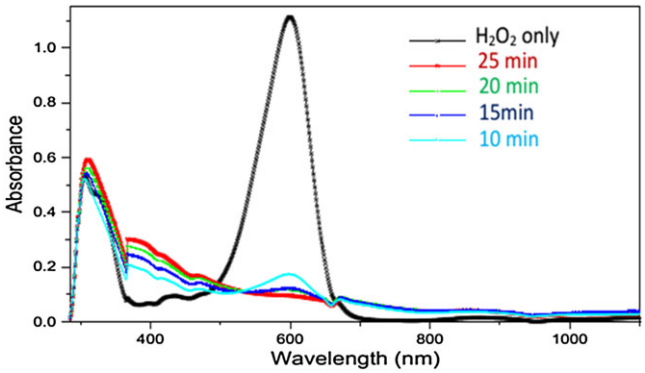

FIGURE 7 Catalytic degradation of indigo carmine by complex 2 at different times

solution without catalysts, a little decay observed in $\lambda_{max} = 625$ nm in the spectrum of the dye. Also, a simple IC degradation in case of using complexes 1 and 3 as catalysts. On contrary, when the complex 2 was introduced, the oxidative reaction was started fast and a gradual vanish of the color of IC is clearly marked. After 10 min from the catalytic reaction the reactivity of catalysts showed the following order 2 > 1 > 3 > H_2O_2 with efficiencies 84.34%, 46.09%, 30.43% and 26.95%, respectively.

The catalytic reactivity of copper complex is higher than nickel and tin complexes may be assigned to the higher redox potential of $Cu^{2+} \rightarrow Cu^{1+} = 0.15$v than $Ni^{2+} \rightarrow Ni^{0} = -0.25$v and $Sn^{2+} \rightarrow Sn^{0} = -0.14$v.[38] On the other hand the lower catalytic activity of the stannous complex is due to the large molecular weight of the complex which reduces the number of the active sites leading to a decreasing of its catalytic activity.[39]

The effect of the complex 2 as catalyst was studied at different times at 10,15, 20 and 25 min. The catalytic efficiency is increased with time, after 25 min from the reaction start, the catalyst efficiency reached to 92.17%, Figure 7.

Where the concentration of the oxidant H_2O_2 was high excess than that of the indigo carmine dye, the catalytic decomposition of the dye is carried out with pseudo-

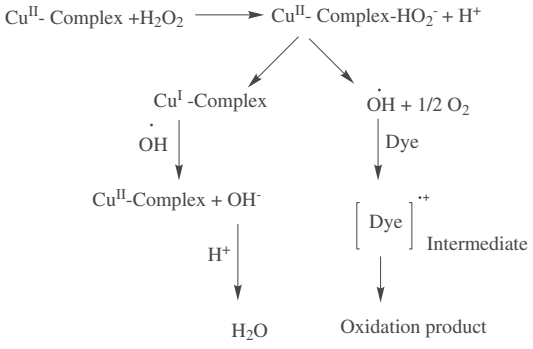

SCHEME 1 Mechanism of redox catalytic degradation of indigo carmine dye

first order reaction with respect to dye concentration. The observed rate constant, $k_0 = 0.093$ min^{-1}, calculated from the slope of the straight lines from the first order kinetic plot using equation 2:-[24].

$$\ln A = \ln A_0 - k_0 wt \quad (2)$$

where A is the absorbance of dye at a definite time t, A_0 is the initial absorbance at $t = 0$, w is the weight of the catalyst, and t is the time of degradation.

3.3 | Mechanism of degradation

It was concluded[40] that the nitrogen donor ligands resulted on destabilization of the Cu^{2+} center and hence raise the potential of Cu^{2+}–Cu^{1+} reduction and the use of π-accepting ligand favors Cu^{1+} state which is required for dye degradation by redox reaction.

It is popularly believed that the redox mechanism, Scheme 1 involves the reduction of Cu^{2+} to Cu^{1+} which facilitate the generation of $OH^{\bullet}$ radicals from H_2O_2 to attack and decompose the indigo carmine dye.[41]

The catalytic removal of IC does not necessarily produces a complete degradation and may be lead to fragmentation without complete mineralization.[42] From figure7, the absorbance increase at 334 nm and 405 nm can be ascribed to IC is converted to isatin sulfonic acid.[43–45]

4 | CONCLUSIONS

Three new nickel, copper and tin Schiff base complexes with different chelation modes and geometrical structures are synthesized and characterized in this work. The catalytic reactivity of the complexes are studied for the oxidative degradation and removal of indigo carmine dye from aqueous solution. The role of the complexes as catalysts was demonstrated. The efficiency of the copper complex is the highest between the other catalysts and its efficiency in decolorization of the dye is found to be 92.17% after 25 min.

ORCID

Amr Mohammad Nassar http://orcid.org/0000-0001-5366-3535

REFERENCES

[1] W. A. Zoubi, A. A. S. Al-Hamadani, M. Kasem, *App. Organomet. Chem.* **2016**, *30*, 810.

[2] E. Kadwa, H. B. Friedrich, M. D. Bala, *Inorg. Chim. Acta* **2017**, *463*, 112.

[3] S. Packianathan, G. Kumaravel, N. Raman, *App. Organomet. Chem.* **2017**, https://doi.org/10.1002/aoc.3577.

[4] H. Zafar, A. Ahmad, A. U. Khan, T. A. Khan, *J. Mol. Str.* **2015**, *1097*, 129.

[5] Z. Liu, F. C. Anson, *Inorg. Chem.* **2001**, *40*, 1329.

[6] A. M. Nassar, A. M. Hassan, A. N. Elkmash, *App. Organomet. Chem.* **2017**, https://doi.org/10.1002/aoc.3572.

[7] S. Suganya, F. P. Xavier, K. S. Nagaraja, *Bull. Mat. Sci.* **1998**, *21*, 403.

[8] W. Al Zoubi, Y. G. Ko, *App. Organomet. Chem.* **2017**, 31, https://doi.org/10.1002/aoc.3574.

[9] A. Ourari, I. Bougossa, S. Bouacida, D. Aggoun, R. R. Rosas, E. Morallon, H. Merazig, *J. Iran. Chem. Soc.* **2017**, *14*, 703.

[10] A. K. Asatkar, M. Tripathi, S. Panda, R. Pande, S. S. Zade, *Spectrochim. Acta. A.* **2017**, *171*, 18.

[11] K. Zhang, A. Gao, C. Zhang, K. Xie, *Desalin. and Water Treatm.* **2016**, *57*, 19190.

[12] W. Jiang, B. Xu, F. Liu, Y. Wang, Z. Xiang, *Synth., React., Inorg., Metalorg., Nanomet., Chem.* **2015**, *45*, 34.

[13] A. S. Elsherbiny, H. A. El-Ghamry, *Int. J. Chem. Kinet.* **2015**, *47*, 162.

[14] S. Farhadi, M. M. Amini, M. Dusek, M. Kucerakova, F. Mahmoudi, *J. Mol. Struc.* **2017**, *1130*, 592.

[15] M. S. Secula, I. Creţescu, S. Petrescu, *Desalination* **2011**, *277*, 227.

[16] C. N. Arenas, A. Vasco, M. Betancur, J. D. Martínez, *Proce. Safe. and Envirom. Protec.* **2017**, *106*, 224.

[17] N. Barka, A. Assabbane, A. Nounah, Y. Aît Ichou, *J. Hazard. Mater.* **2008**, *152*, 1054.

[18] I. A. Salem, H. A. El-Ghamry, M. A. El-Ghobashy, *Beni - Suif University Journal Of Basic and Applied Sciences* **2014**, *3*, 186.

[19] P. Forlano, J. A. Olabe, J. F. Magallanes, M. A. Blesa, *Canad. J. Chem.* **1997**, *75*, 9.

[20] L. Cheng, M. Wei, L. Huang, F. Pan, D. Xia, X. Li, A. Xu, *Ind. Eng. Chem. Res.* **2014**, *53*, 3478.

[21] M. B. Kasiri, A. R. Khataee, *Env. Tech.* **2012**, *33*, 1417.

[22] Y. X. Penga, X. L. Zhaoa, D. Xua, H. F. Qianb, W. Huanga, *Dyes Pigm.* **2017**, *136*, 559.

[23] A. H. Gemeay, I. A. Mansour, R. G. El-Sharkawy, A. B. Zaki, *J. Molec. Cat. A: Chem.* **2003**, *193*, 109.

[24] K. El-Baradie, R. El-Sharkawy, H. El-Ghamry, K. Sakai, *Spectrochim. Acta. A.* **2014**, *121*, 180.

[25] H. El-Ghamry, R. El-Sharkawy, M. Gaber, *J. Iran. Chem. Soc.* **2014**, 11,379.

[26] N. M. Ibrahim, H. A. A. Yosef, E. F. Ewies, M. R. H. Mahran, M. M. Alib, A. E. Mahmoud, *J. Braz. Chem. Soc.* **2015**, *26*, 1086.

[27] S. S. Kandil, A. El-Dissouky, G. Y. Ali, *J. Coord. Chem.* **2004**, *57*, 105.

[28] O. F. Ozturk, A. Cansiz, M. Koparir, *Trans. Met. Chem.* **2007**, *32*, 224.

[29] A. M. Hassan, A. M. Nassar, Y. Z. Hussien, A. N. Elkmash, *App. Biochem., Biotech.* **2012**, *167*, 58.

[30] K. Nakamoto, *Infrared and Raman Spectra of Inorganic and Coordination Compounds*, Wiley, New York **1986**.

[31] A. M. Nassar, A. M. Hassan, S. S. Al-Abd, *Synth., React., Inorg., Metalorg., Nanomet., Chem.* **2015**, *45*, 3256.

[32] A. Varshney, J. P. Tandon, *Polyhedron* **1986**, *5*, 1853.

[33] A. C. Fellah, J. Meullemeestre, C. Spies, F. Vierling, M. A. Khan, *Trans. Met. Chem.* **1999**, *24*, 135.

[34] A. M. A. Alaghaz, B. A. El-Sayed, A. A. El-Henawy, R. A. A. Ammar, *J. Mol. Str.* **2013**, *1035*, 83.

[35] H. L. Singh, J. B. Singh, S. Bhanuka, *J. Coord. Chem.* **2015**, *69*, 343.

[36] D. Arish, M. S. Nair, *J. Mol. Str.* **2010**, *983*, 112.

[37] Z. Hong-Yun, C. Dong-Li, C. Pei-Kun, C. De-Ji, C. Guang-Xia, Z. Hong-Quan, *Polyhedron* **1992**, *11*, 2313.

[38] A. J. Bard, R. Parsons, J. Jordan, *Standard Potentials in Aqueous Solutions*, Marcel Dekker, New York **1985**.

[39] R. G. El-Sharkawy, A. S. Badr El-din, S. E. H. Etaiw, *Spectrochim. Acta. A* **2011**, *79*, 1969.

[40] T. K. Lal, J. R. Richardson, M. S. Mashuta, R. M. Buchanan, R. Mukherjee, *Polyhedron* **1997**, *16*, 4331.

[41] S. H. Tiana, Y. T. Tu, D. S. Chena, X. Chena, Y. Xionga, *Chem. Eng. J.* **2011**, *169*, 31.

[42] A. H. Gemeay, M. E. El-Halwagy, R. G. El-Sharkawy, A. B. Zaki, *J. Environ. Chem. Eng.* **2017**, *5*, 2761.

[43] A. J. Kettle, B. M. Clark, C. C. Winterbourn, *J. Biol. Chem.* **2004**, *279*, 18521.

[44] T. T. Blancas, G. R. Morales, F. U. Núñez, C. B. Díaz, A. D. González, R. Natividad, *J. Taiw. Inst. Chem. Eng.* **2017**, *74*, 225.

[45] M. Bernal, R. Romero, G. Roa, C. B. Díaz, T. T. Blancas, R. Natividad, *Int. J. Photoenergy* **2013**, 7.

How to cite this article: Nassar AM. Catalytic reactivity of new Ni(II), cu(II) and Sn(II) complexes for decolorization of indigo carmine in aqueous solution, high efficiency of copper complex. *Appl Organometal Chem*. 2017;e4056. https://doi.org/10.1002/aoc.4056